DOI: 10.1002/anie.201203374

Fluorescent Nanoparticles

White Fluorescence from Core–Shell Silica Nanoparticles**

Jeremy Malinge, Clémence Allain,* Arnaud Brosseau, and Pierre Audebert*

Silica nanoparticles (NPs) are versatile materials with unique properties. Since the first reports of their colloidal fabrication[1,2] and functionalization[3–5] with light-emitting molecules, their photophysical properties have been extensively studied.[6,7] One of the most fascinating advances in this area of research deals with the incorporation of multiple dyes in one nanoparticle, which allows the formation of ultrabright nanoobjects.[8] From the accumulation of different photoresponsive molecules inside the silica core, complex photophysical events may arise, such as excimer formation,[9,10] photoswitchable fluorescence emission,[11] or resonance energy transfer.[12,13] As a result, new luminescent nanoobjects with multiple color emission under a single excitation wavelength are accessible and find applications in sensors,[14,15] biolabeling,[16] and emitting displays.

In the meantime, much attention has been directed to the fabrication of white-light-emitting devices. In most devices, the white fluorescence arises from the mixing of various dyes having blue, green, and orange fluorescence simultaneously.[17–22] Such displays require a careful control of each color contribution and of the energy transfer between the different dyes to obtain the pure white color according to the CIE standards. This issue has been overcome by Park et al.[23] by blocking any energy transfer between two linked fluorophores with blue and yellow emission. Multiple dye-doped silica NPs may be an interesting alternative to prepare such white displays, as many different light-emitting fluorophores can be hosted in the same unit.

s-Tetrazines are aromatic heterocycles that have a structure similar to a benzene ring, where four carbon atoms are replaced by nitrogen. We[24] and others[25] have explored the photophysical and electrochemical properties of these molecules. Indeed, some tetrazines substituted with heteroatoms[26] showed a high fluorescence quantum yield, a good photostability, and a long fluorescence lifetime. Furthermore, s-tetrazines are extremely electron-deficient and can be reversibly reduced, leading to nonfluorescent species.[27] These photophysical and electrochemical properties make these fluorophores attractive candidate for sensing purposes.[28] In a recent study, we attached tetrazine derivatives onto the surface of silica nanoparticles and evaluated the sensing properties of these nanoobjects.[29] Another recent study from our group[30] showed that a naphthalimide chromophore covalently linked to a tetrazine was able to act as an antenna, increasing the brightness of the tetrazine. Herein we report a new white-light-emitting system based on bichromophoric silica NPs doped by a naphthalimide dye in the inner core and by a tetrazine derivative on the outer shell.

Reaction between 1,8-naphthalic anhydride and ethanolamine provided N-(hydroxyethyl)-1,8-naphthalimide **1** rapidly and in good yield. Intermediate **1** was reacted with triethoxy(3-isocyanatopropyl)silane, providing the desired silane-functionalized naphthalimide derivative (designated Napht). The corresponding tetrazine derivative was obtained as described in our previous study (Scheme 1; see also the Supporting Information).

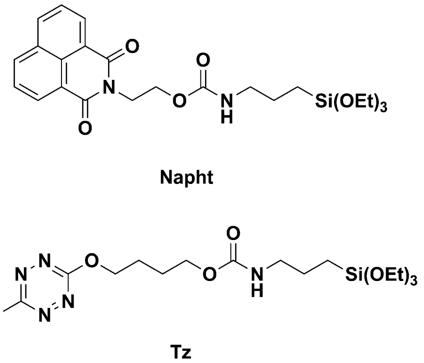

Scheme 1. Naphthalimide (Napht) and tetrazine (Tz) derivatives.

The co-functionalized NPs are prepared in two steps. First, the naphthalimide dye is incorporated inside the silica matrix following an existing method,[12] which involves the prehydrolysis of Napht before the onset of colloid formation, to provide naphthalimide doped silica nanoparticles (denoted NP0). After the reaction, the samples were washed by successive centrifugations and redispersions in dry CH_3CN. The NPs thus obtained present a diameter of 80 nm measured by dynamic light scattering (DLS). A value of 0.18 mmol of Napht per gram of silica was calculated from TGA. In the second step, a NP0 suspension in dry CH_3CN is reacted with the dye Tz in the presence of acetic acid, as described in our previous work.[29]

Aliquots of the grafting reaction mixture were isolated after 2, 24, and 40 h, providing three different sets of NPs, which are respectively denoted NPA, NPB, and NPC. The amount of tetrazine grafted as well as the DLS size distributions are shown in Table 1.

The photophysical properties of the new silane derivative Napht were investigated in CH_3CN. The absorption spectrum

---

[*] J. Malinge, Dr. C. Allain, A. Brosseau, Prof. P. Audebert
PPSM, CNRS UMR 8531, Ecole Normale Supérieure de Cachan
61, avenue du Président Wilson, 94235 Cachan cedex (France)
E-mail: clemence.allain@ppsm.ens-cachan.fr
audebert@ppsm.ens-cachan.fr

[**] This work was supported by the DGA (Direction Générale de l'Armement) for a Ph.D. to J.M. Many thanks to Dr. Gilles Clavier and Dr. Rachel Méallet-Renault for fruitful discussions.

Supporting information for this article is available on the WWW under http://dx.doi.org/10.1002/anie.201203374.

Table 1: Diameter and composition of the nanoparticles.

System	Reaction time [h]	Diameter[a]	Dye loading[b] [mmol g^{-1}]
NP0	initial	77	0.180/0
NPA	2	96	0.180/0.035
NPB	24	97	0.180/0.083
NPC	40	102	0.180/0.092

[a] Measured by DLS. [b] Loading of Napht/Tz was measured by TGA.

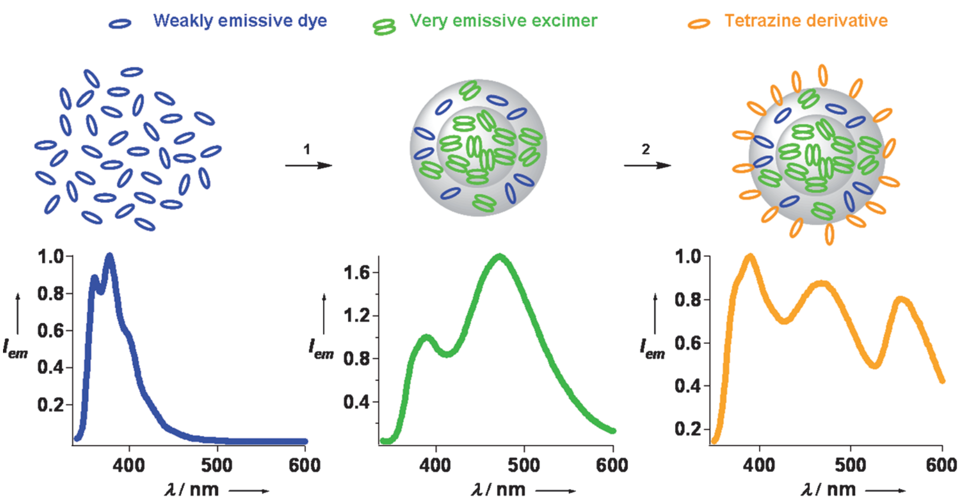

Figure 1. Representation of the co-grafting process: 1) formation of NP0; 2) Tz grafting reaction. Emission spectra ($\lambda_{exc} = 330$ nm) of Napht (blue), NP0 (green), and NPB (orange).

shows two bands at 332 and 344 nm and the emission spectrum shows two weak (quantum yield 2.9%) fluorescent bands at 361 and 377 nm that are characteristic of naphthalimide derivatives (Supporting Information, Figure S3).

The fluorescence decay is monoexponential, with a lifetime of 0.28 ns. Those values match all previously reported data on such molecules. The tetrazine moiety presents two weak absorption bands at 330 and 515 nm together with a large fluorescence band at 565 nm (quantum yield 26%) with a long fluorescence lifetime (148 ns). Again, those properties are typical of chloroalkoxytetrazines compounds.

In contrast with the free dye in solution, the new NP0 system presents two well-separated emission bands at 390 and 472 nm. The excitation spectra at 472 nm matches the absorbance spectra of the chromophore Napht in solution (Supporting Information, Figure S5), suggesting the formation of a very emissive excimer. The fluorescence decay of the first emission band (390 nm) exhibits an average lifetime of 0.79 ns, while the excimeric band shows a much longer average fluorescence lifetime of 19.74 ns. The overall fluorescence quantum yield of this new hybrid system reaches 20%. Excimer formation has already been described in the case of two naphthalimide moieties linked by an aliphatic chain,[31,32] but the intensity of the excimeric band never exceeds the single molecule emission. In our system, the encapsulation of Napht inside silica greatly favors the formation of excimers and strongly enhances their fluorescence.

The steady-state fluorescence spectra of NPA, NPB, and NPC (Figure 1; Supporting Information, Figure S4) all present a new fluorescence band centered at 565 nm, which corresponds to the emission of the tetrazine moiety. The photostability of this sytem is comparable to a tetrazine covalently linked to a naphthalimide(NITZ)[30] (Supporting Information, Figure S12) and is noticeably better than the one of the parent N-(hydroxyethyl)-1,8-naphthalimide. Fluorescence decay in the tetrazine emission band can be fitted by a bi-exponential decay, with an average fluorescence lifetime varying between 25 and 30 ns for NPA, NPB, or NPC. With time, the yellow fluorescence increases as more tetrazine is grafted onto the silica surface (Supporting Information, Figure S4). In the meantime, the fluorescence intensity of the excimeric band decreases drastically. A close look at the fluorescence excimeric band and at the n–π* absorption band of the tetrazine reveals a strong spectral overlap meaning that a fluorescence energy transfer (FRET) is possible between the naphthalimide excimer (donor) and the tetrazine (acceptor). This is confirmed by the excitation spectrum of NPC at 565 nm (tetrazine fluorescence), which shows contributions from tetrazine and naphthalimide absorptions (Supporting Information, Figure S6). Furthermore, excitation of NPC at 355 nm (donor only) provides the tetrazine fluorescence (Figure 2). Meanwhile, the quantum yield of the excimeric band decreases from 12.4% to 3.9% upon tetrazine grafting, and its average fluorescence lifetime decreased from 19.74 to 7.87 ns (Table 2). Finally, careful examination of the fluorescence decay of NPB ($\lambda_{exc} = 360$ nm, $\lambda_{em} = 600$ nm; Supporting Information, Figure S10) reveals a rise time of 0.53 ns, which further confirms the energy transfer. Altogether, this confirms there is an energy transfer between the naphthalimide excimer and the tetrazine enhancing the brigthness of the tetrazine. The quantum

Table 2: Spectroscopic properties of the NP and the excimer.

System	Global Φ_F	Excimer Φ_F[a]	Excimer lifetime [ns]
NP0	0.20	0.124	19.74
NPA	0.21	0.098	14.30
NPB	0.17	0.062	9.00
NPC	0.16	0.039	7.87

[a] defined as the ratio of the number of photons emitted in this band ($430 < \lambda < 520$ nm) and the number of photons absorbed ($\lambda_{exc} = 330$ nm).

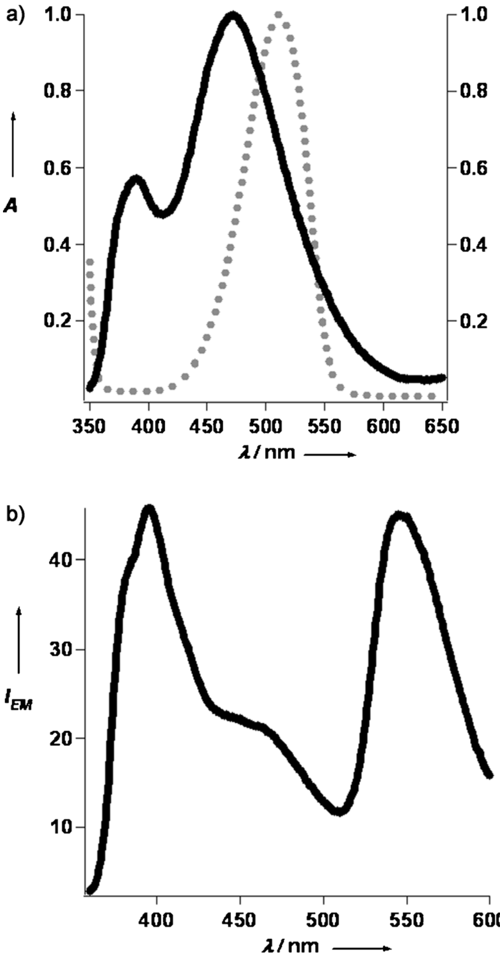

Figure 2. a) Spectral overlap between NP0 emission (donor, full line) and Tz absorption (dotted lines). b) Emission spectra of NPC ($\lambda_{exc}=355$ nm, donor only).

yield of the bichromophoric NPs decreases slightly from 0.21 to 0.16 between NPA and NPC: the intermolecular quenching between grafted tetrazines that was observed in our previous work[29] remains limited in this new system. Indeed, while silica NPs grafted only with Tz exhibit a fluorescence quantum yield of 2.7 % the quantum yield of NPB under 515 nm excitation (excitation of Tz only, neither Napht nor excimer contribution) reaches 4.8 %.[33] Apart from being FRET donors, the naphthalimide on the surface of the NPs may act as spacers, decreasing the intermolecular quenching between tetrazines and thus affording a brightly emissive system.

Such energy transfer in the couple tetrazine–naphthalimide has already been described by us. Indeed, there is a small spectral overlap between the emission band of the naphthalimide free dye and the n–π^* transition of the tetrazine, leading to a mixed Förster–Dexter energy transfer type when the two chromophores are covalently linked.[30]

In our system, the spectral overlap is greatly enhanced by the formation of the naphthalimide excimer, the emission of which is red-shifted. We suggest that a long range energy transfer is therefore possible between tetrazines on the surface of the nanoparticles and encapsulated excimers close to the surface. Calculation of the Förster radius for this FRET pair gives a value of 1.7 nm (for calculation details, see the Supporting Information). This distance is short compared to the nanoparticle radius (50 nm), which explains why the excimeric band is still persistent even after 40 h of grafting on the surface: the excimeric rich core is too far from the surface for an efficient energy transfer to occur.

Upon UV irradiation (330 nm), the co-functionalized system exhibits a change of color emission along with the increasing amount of tetrazine linked on its surface. The tetrazine free dye exhibits in acetonitrile a deep yellow color ($x=0.47$, $y=0.52$) located on the yellow edge of the 1931 CIE chromaticity diagram (Figure 3). On the other hand, under UV irradiation, suspensions of NP0 in acetonitrile provide a green fluorescence ($x=0.16$, $y=0.19$) on the other edge of the diagram. With an increasing quantity of tetrazine grafted, our nanoparticles gradually change their photoluminescence to a pure white emission ($x=0.29$, $y=0.32$).

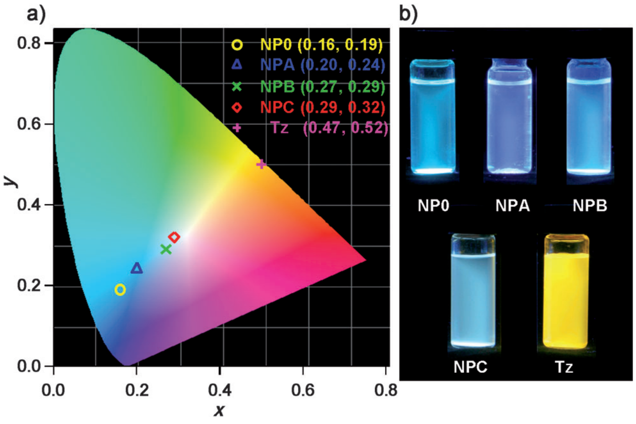

Figure 3. a) Emission colors in a CIE 1931 chromaticity diagram; ideal white: $x=0.33$, $y=0.33$. b) Suspensions of NPs in CH_3CN ($\lambda_{exc}=365$ nm, UV lamp).

This white photoluminescence arises from the addition of the contributions of three different emitting species. The blue emission comes from the free naphthalimide dyes still emitting at 390 nm. The remaining excimers, which cannot be quenched by tetrazine, are shielded inside the silica core and still emit a green fluorescence centered at 472 nm. Finally, the tetrazines grafted on the surface of the nanospheres provide the last yellow contribution.

In summary, the encapsulation of silane-appended naphthalimide Napht in the core of silica NPs afforded highly emissive monodisperse nanospheres with a strong green excimeric emission, together with the blue emission of the monomeric naphthalimide. A tetrazine derivative was then grafted on the surface of these NPs. Energy transfer between naphthalimide excimers and tetrazines is observed, enhancing the brightness of the tetrazine acceptors. The added contributions of the monomeric emitter (blue fluorescence) together with the green emitting excimeric core and the yellow fluorescence of tetrazine provides new bichromophoric silica nanoparticles displaying an intense ($\varphi = 0.16$) pure white ($x = 0.29$, $y = 0.32$) fluorescence emission.

Received: May 2, 2012
Revised: June 8, 2012

Keywords: energy transfer · naphthalimide · silica nanoparticles · tetrazine · white fluorescence

---

[1] W. Stöber, A. Fink, E. Bohn, *J. Colloid Interface Sci.* **1968**, *26*, 62.
[2] A. van Blaaderen, A. Vrij, *J. Colloid Interface Sci.* **1993**, *156*, 1–18.
[3] A. Van Blaaderen, A. Vrij, *Langmuir* **1992**, *8*, 2921–2931.
[4] R. Nyffenegger, C. Quellet, J. Ricka, *J. Colloid Interface Sci.* **1993**, *159*, 150–157.
[5] N. A. M. Verhaegh, A. Vanblaaderen, *Langmuir* **1994**, *10*, 1427–1438.
[6] H. Goesmann, C. Feldmann, *Angew. Chem.* **2010**, *122*, 1402–1437; *Angew. Chem. Int. Ed.* **2010**, *49*, 1362–1395.
[7] S. Bonacchi, D. Genovese, R. Juris, M. Montalti, L. Prodi, E. Rampazzo, N. Zaccheroni, *Angew. Chem.* **2011**, *123*, 4142–4152; *Angew. Chem. Int. Ed.* **2011**, *50*, 4056–4066.
[8] H. Ow, D. R. Larson, M. Srivastava, B. A. Baird, W. W. Webb, U. Wiesner, *Nano Lett.* **2005**, *5*, 113–117.
[9] P. J. Dewar, T. F. MacGillivray, S. M. Crispo, T. Smith-Palmer, *J. Colloid Interface Sci.* **2000**, *228*, 253–258.
[10] E. Rampazzo, S. Bonacchi, M. Montalti, L. Prodi, N. Zaccheroni, *J. Am. Chem. Soc.* **2007**, *129*, 14251–14256.
[11] F. May, M. Peter, A. Hütten, L. Prodi, J. Mattay, *Chem. Eur. J.* **2012**, *18*, 814–821.
[12] L. Wang, W. Tan, *Nano Lett.* **2006**, *6*, 84–88.
[13] M. Montalti, L. Prodi, N. Zaccheroni, A. Zattoni, P. Reschiglian, G. Falini, *Langmuir* **2004**, *20*, 2989–2991.
[14] D. Gao, Z. Wang, B. Liu, L. Ni, M. Wu, Z. Zhang, *Anal. Chem.* **2008**, *80*, 8545–8553.
[15] B. Liu, F. Zeng, G. Wu, S. Wu, *Chem. Commun.* **2011**, *47*, 8913–8915.
[16] T. Doussineau, A. Schulz, A. Lapresta-Fernandez, A. Moro, S. Körsten, S. Trupp, G. J. Mohr, *Chem. Eur. J.* **2010**, *16*, 10290–10299.
[17] G. M. Farinola, R. Ragni, *Chem. Soc. Rev.* **2011**, *40*, 3467–3482.
[18] M. Melucci, M. Zambianchi, G. Barbarella, I. Manet, M. Montalti, S. Bonacchi, E. Rampazzo, D. C. Rambaldi, A. Zattoni, P. Reschiglian, *J. Mater. Chem.* **2010**, *20*, 9903–9909.
[19] E.-J. Park, T. Erdem, V. Ibrahimova, S. Nizamoglu, H. V. Demir, D. Tuncel, *ACS Nano* **2011**, *5*, 2483–2492.
[20] S. S. Babu, J. Aimi, H. Ozawa, N. Shirahata, A. Saeki, S. Seki, A. Ajayaghosh, H. Möhwald, T. Nakanishi, *Angew. Chem.* **2012**, *124*, 3447–3451; *Angew. Chem. Int. Ed.* **2012**, *51*, 3391–3395.
[21] A. H. Shelton, I. V. Sazanovich, J. A. Weinstein, M. D. Ward, *Chem. Commun.* **2012**, *48*, 2749–2751.
[22] C. Y. Hsu, Y. L. Liu, *Chem. Eur. J.* **2011**, *17*, 5522–5525.
[23] S. Park, J. E. Kwon, S. H. Kim, J. Seo, K. Chung, S.-Y. Park, D.-J. Jang, B. Medina, J. Gierschner, S. Y. Park, *J. Am. Chem. Soc.* **2009**, *131*, 14043–14049.
[24] G. Clavier, P. Audebert, *Chem. Rev.* **2010**, *110*, 3299–3314.
[25] F. Gückel, A. H. Maki, F. A. Neugebauer, D. Schweitzer, H. Vogler, *Chem. Phys.* **1992**, *164*, 217–227.
[26] Y.-H. Gong, F. Miomandre, R. Méallet-Renault, S. Badré, L. Galmiche, J. Tang, P. Audebert, G. Clavier, *Eur. J. Org. Chem.* **2009**, 6121–6128.
[27] F. Miomandre, E. Lépicier, S. Munteanu, O. Galangau, J. F. Audibert, R. Méallet-Renault, P. Audebert, R. B. Pansu, *ACS Appl. Mater. Interfaces* **2011**, *3*, 690–696.
[28] P. Audebert, F. Miomandre, G. Clavier, M.-C. Vernières, S. Badré, R. Méallet-Renault, *Chem. Eur. J.* **2005**, *11*, 5667–5673.
[29] J. Malinge, C. Allain, L. Galmiche, F. Miomandre, P. Audebert, *Chem. Mater.* **2011**, *23*, 4599–4605.
[30] Q. Zhou, P. Audebert, G. Clavier, R. Méallet-Renault, F. Miomandre, J. Tang, *New J. Chem.* **2011**, *35*, 1678–1682.
[31] D. W. Cho, M. Fujitsuka, A. Sugimoto, T. Majima, *J. Phys. Chem. A* **2008**, *112*, 7208–7213.
[32] T. C. Barros, P. B. Filho, V. G. Toscano, M. J. Politi, *J. Photochem. Photobiol. A* **1995**, *89*, 141–146.
[33] In the case of multiple-dye-doped silica NPs, the fluorescence quantum yield depends on the excitation wavelength: here, upon 330 nm excitation, the fluorescence emission arises from Napht, excimer, and Tz (through direct excitation and FRET), while upon 515 nm excitation, the fluorescence emission is due to Tz only (direct excitation). In the UV region (330–360 nm), the quantum yield dependence with the excitation wavelength is below the experimental error (+/−10%) for quantum yield measurements.